arXiv:0704.0428v1 [astro-ph] 3 Apr 2007

Star Formation in the Bok Globule CB 54

David R. Ciardi

Michelson Science Center/Caltech
770 South Wilson Avenue, M/S 100-22
Pasadena, CA 91125

`ciardi@ipac.caltech.edu`

Cynthia Gómez Martín

University of Florida, Department of Astronomy
211 Bryant Space Sciences Building, Gainesville, FL 32611

`gomez@astro.ufl.edu`

ABSTRACT

We present mid-infrared (10.4 μm, 11.7 μm, and 18.3 μm) imaging intended to locate and characterize the suspected protostellar components within the Bok globule CB54. We detect and confirm the protostellar status for the near-infrared source CB54YC1-II. The mid-infrared luminosity for CB54YC1-II was found to be $L_{midir} \approx 8\ L_{\odot}$, and we estimate a central source mass of $M_{*} \approx 0.8\ M_{\odot}$ (for a mass accretion rate of $\dot{M} = 10^{-6}\ M_{\odot}\ yr^{-1}$). CB54 harbors another near-infrared source (CB54YC1-I), which was not detected by our observations. The non-detection is consistent with CB54YC1-I being a highly extinguished embedded young A or B star or a background G or F giant. An alternative explanation for CB54YC1-I is that the source is an embedded protostar viewed at an extremely high inclination angle, and the near-infrared detections are not of the central protostar, but of light scattered by the accretion disk into our line of sight. In addition, we have discovered three new mid-infrared sources, which are spatially coincident with the previously known dense core in CB54. The source temperatures ($\sim$ 100K) and association of the mid-infrared sources with the dense core suggests that these mid-infrared objects may be embedded class 0 protostars.

Subject headings: infrared: ISM — infrared: stars — ISM: globules — ISM: individual (CB54, LBN 1042) — stars: formation — stars: pre–main-sequence

1. Introduction

Protostars are young stellar objects that are still in the process of accreting the bulk of their material. Class 0 sources have been proposed as the evolutionary precursors to the class I protostars (André, Ward-Thompson, & Barsony 1993; André & Montmerle 1994). Work by Bontemps et al. (1996) and Saraceno et al. (1996) suggested a direct evolutionary sequence from the class 0 stage to the class I stage. However, Jayawardhana, Hartmann, & Calvet (2001) have argued that class 0 protostars are located preferentially in higher density regions and that class I young stellar objects are located preferentially in lower density regions and, thus, may be at a comparable evolutionary states. To further complicate the distinction between class 0 and class I objects, some class I objects, which are viewed at high inclination, may appear "class 0-like" because of the high optical depth associated with viewing the disk (nearly) edge-on (Masunaga & Inutsuka 2000).

An example of this confusion may be seen in the binary system L1448N(A,B), where one component of the system has the spectral energy distribution (SED) of a class 0 protostar while the other has an SED of a class I protostar (Ciardi et al. 2003; O'Linger et al. 2006). This spread in apparent evolutionary status is also seen in larger clusters. In Perseus, Rebull et al. (2007) found that sources within clusters exhibited SEDs for a wide range in circumstellar environments, suggesting class 0 to class II protostars within the same aggregate. Either viewing geometry plays a significant role in our interpretation for each of the SEDs, the aggregates span a significant age spread, or if the sources are coeval, the disks/envelopes evolve faster than anticipated.

To help address these issues, it would be beneficial to study a set of young stellar objects, located within the same environment, but isolated and free from the influence of other active star formation. The Bok Globule CB54, known to be a site of active star formation, may provide such an environment of isolated aggregate star formation.

CB54 (LBN 1042; Clemens & Barvainis 1988) is a $\sim 100\ M_{\odot}$ Bok globule associated with the Vela OB1 molecular cloud (d≈1500 pc; Launhardt & Henning 1997; Launhardt, Ward-Thompson, 1997). Bok globules are small (10−100 $M_{\odot}$; Clemens, Yun, & Heyer 1991), isolated molecular clouds, most of which have been identified via opaque patches in optical images (Clemens & Barvainis 1988; Bourke, Hyland, & Robinson 1995). Globules have been found to be sites of star formation (e.g., Yun & Clemens 1990, 1994a,b; Alves & Yun 1995; Moreira & Yun 1995), of both single low-mass stars and multiple or binary stars (e.g., Yun 1996).

Active star formation in CB54 was first identified by the association of a dense core with the IRAS point source PSC 07020-1618, which is located at the center of a collimated molecular outflow (Yun & Clemens 1994b). Near-infrared imaging revealed that CB54 actually contains two bright near-infrared sources (CB54YC1-I, CB54YC1-II) and diffuse nebulosity of shocked H_2 emission connecting the two sources (see Figure 1 and Yun 1996; Khanzadyan 2003). The positions of CB54YC1-I and -II are offset from the position of the IRAS point source (see Figure 1), although the IRAS beam size and PSC positional errors ($20'' \times 4''$) do make it difficult to associate any one source with IRAS 07020-1618.

Based upon its near-infrared colors ($J-K = 5.29$ mag, $H-K = 2.58$ mag), CB54YC1-II was classified as a class I young stellar object (Yun 1996). There is an MSX point source (G228.9946-04.6200), detected only in Band-A (8.3 μm), within a few arcsecs of CB54YC1-II (see Figure 1). CB54YC1-I ($J-K = 4.34$ mag, $H-K = 1.63$ mag) was also classified as a class I protostar (Yun 1996), but despite its similar near-infrared brightness to CB54YC1-II, it was not detected by MSX. Unlike CB54YC1-II, the near-infrared colors of CB54YC1-I could be explained with a highly extinguished ($A_V \sim 20$ mag) "bare" photosphere. VLA observations detected a 3.6 cm and 6 cm source within a few arcseconds of CB54YC1-I (see Figure 1), possibly indicating a stellar wind or accretion shock (Yun et al. 1996; Moreira et al. 1997).

The position of the IRAS point source is spatially coincident with a dense core revealed in sub-mm, mm, and molecular line mapping; the position of which is offset from the positions of CB54YC1-I and CB54YC1-II but coincident with the IRAS point source (see Figure 1 and e.g., Wang et al. 1995; Zhou, Evans, & Wang 1996; Henning et al. 2001). Molecular line observations also indicated the presence of gravitational collapse in the core of CB54 (Wang et al. 1995; Afonso, Yun, & Clemens 1998). Water maser emission, almost exclusively associated with class 0 protostars in regions of low-mass star formation (e.g., Furuya et al. 2001), was also discovered in CB54 (de Gregorio-Monsalvo et al. 2006; Gómez et al. 2006). All of this suggests that the star formation in CB54 may be more substantial than revealed by the near-infrared imaging alone.

We have observed the mid-infrared emission from the Bok globule CB54 at high spatial resolution ($\sim 0\farcs5$) to clarify the evolutionary status of CB54YC1-I and CB54YC1-II and to search for additional protostars embedded in the globule core. Our work confirms the protostellar status of CB54YC1-II, but indicates that CB54YC1-I may be a more evolved young stellar object or a background giant star. In addition, we have discovered three new mid-infrared sources which are spatially coincident with the dense core and may be class 0 protostars.

2. Observations and Data Reduction

Mid-infrared imaging observations of CB54 were made on 2004 February 01 (UT) using the Thermal Region Camera and Spectrograph (T-ReCS; Telesco et al. 1998) on the Gemini South 8 m telescope. T-ReCS utilizes a 320×240 pixel Si:As blocked impurity band detector, with a spatial scale of $0\farcs089$ pixel^{-1} and a field of view of $28\farcs8 \times 21\farcs6$. The observations were centered on the J2000 coordinates $(\alpha, \delta) = (\alpha = 07h04m21s,\ \delta = -16°23'19'')$. Imaging was obtained in three filters (N, Si-11.7 and Qa-18.3). The on-sky alignment of the T-ReCS field-of-view was chosen to cover the entire near-infrared nebulosity, the two known near-infrared sources, and the peak of the sub-millimeter (850 μm) core (see Figure 1).

A standard off-chip $15''$ north-south chop-nod sequence was employed with total on-source integration times of 300 s per image. Three exposures in the Qa-18.3 filter were acquired for a total on-source integration time of 900 s. Flux calibration was obtained from imaging of the standard star HD 32887 (see the Gemini webpage for a compilation of mid-infrared standard stars and flux densities.)[1]. The weather quality was listed as the 50th-percentile, and the seeing at 11.7 μm was $\approx 0\farcs4$. A summary of the filters, frame times, total integration time per filter, and associated air masses is given in Table 1.

The data were reduced with custom-written IDL routines for the T-ReCS data format. Four mid-infrared sources were detected by our observations, with no evidence of extended or diffuse mid-infrared emission (see Figure 2). Standard aperture photometry was performed using a $1''$ aperture radius. Detection limits were tested by inserting fake sources into the images and performing aperture photometry. A summary of the photometry (including estimated 1σ upper limits) and relative positional offsets with respect to CB54YC1-II is given in Table 2.

3. Discussion

The near-infrared source CB54YC1-II is the brightest mid-infrared source and is detected in each of the mid-infrared filters. The other near-infrared source CB54YC1-I was not detected in any of the mid-infrared imaging. In addition, three new mid-infrared sources have been detected (MIR-a, MIR-b, and MIR-c). MIR-a and MIR-b were detected in each of three mid-infrared filters, while MIR-c was detected only at 18.3 μm. In the following sections, we evaluate the properties of these sources and discuss the possible star formation history of the globule.

---

[1] http://www.gemini.edu/sciops/instruments/mir/MIRPhotStandards.html

3.1. CB54YC1-II

CB54YC1-II, originally classified as a candidate class I protostar (Yun 1996), has a $2.2 - 10.3$ μm spectral index $[\alpha = -d \log(\nu F_\nu)/d \log(\nu)]$ of $\alpha = 0.34 \pm 0.01$, which is consistent with the spectral index expected for a class I/flat spectrum young stellar object. The SED of CB54YC1-II in Figure 3. For comparison, the SED for a confirmed class I young stellar object (IRAS 04195+2251; Eisner, J. et al. 2006), with a similar spectral index $\alpha_{(2.2-10.6\ \mu\mathrm{m})} \approx 0.3$, has been scaled to the SED of CB54YC1-II (see Figure 3), exhibiting good agreement between the SEDs.

If the mid-infrared emission is primarily the result of gravitational infall, (e.g., Ciardi et al. 2003), the mid-infrared luminosity provides a means of estimating the central protostellar mass. Integrating the SED from $1 - 20$ μm, we estimate the mid-infrared luminosity to be $L_{midir} \approx 8 \pm 2\ L_\odot$, for an assumed distance of 1500 pc. We estimate a central source mass from the relation $L = (G\dot{M}M_*)/R_*$, where $\dot{M}$ is the mass infall rate, R_* is the source size, and M_* is the source mass (Shu, Adams, & Lizano 1987). Using a standard $R_* = 3\ R_\odot$ protostellar radius (Stahler, Shu, & Taam 1980) and typical mass accretion rates of $\dot{M} = 10^{-5} - 10^{-6}\ M_\odot\ \mathrm{yr}^{-1}$ (Kenyon, Calvet, & Hartmann 1993), we estimate the central protostellar mass for CB54YC1-II to be $M_* = 0.08 - 0.8\ M_\odot$.

A class II pre-main sequence star located behind a wall of extinction could also explain the observed SED for CB54YC1-II. In Figure 3, a median SED for T Tauri stars (TTS) (D'Alessio et al. 1999) has been scaled and convolved with an extinction model (R=3.1 assumed, Mathis 1990). In order to match both the mid-infrared flux densities and the slope of the near-infrared, the TTS SED must be extinguished by $A_V \approx 25$ magnitudes, and indeed, the position of CB54YC1-II in a JHK color-color ($J - H = 2.71$ mag, $H - K = 2.58$ mag) diagram is consistent with a heavily extinguished TTS (see Figure 4 in Haisch et al. 2000).

The average volume density of the CB54 envelope (i.e., not including the central condensation which is offset from the near-infrared sources), as derived from sub-mm (450 & 850 μm) imaging, is $\langle n_H \rangle \approx 5 \times 10^4\ \mathrm{cm}^{-3}$ (Henning et al. 2001). At 1500 pc, the projected linear radius of the CB54 envelope is $r \approx 22500$ AU ($\approx 15''$). If we assume the globule is spherical, we can derive a peak column density of $N_H \approx 4 \times 10^{22}\ \mathrm{cm}^{-2}$, which corresponds to a visual extinction of $A_V \approx 20$ mag. The extinction estimatation does not take into account specific structure within the cloud including any dense envelope which may immediately surround the source, but does indicate the above derived extinction levels for CB54YC1-II are possible. Without a more complete SED or spectroscopy, especially at $3 - 8$ μm, it is difficult to distinguish between the class I and class II models for CB54YC1-II

3.2. CB54YC1-I

CB54YC1-I was not detected in any of the three mid-infrared images, calling into question the original class I protostellar classification. Scaling the SED for the class I protostar (IRAS 04295+2251) to the JHK SED of CB54YC1-I, the predicted mid-infrared flux densities for CB54YC1-I are $F_\nu \sim 80 - 100$ mJy at 11.7 μm and $F_\nu \sim 150$ mJy at 18.3 μm. The predicted emission is $\sim 10\sigma$ above the detection limits (see Figure 4.

The JHK slope for CB54YC1-I is too steep to match the near-infrared SED for a class II (TTS) pre-main sequence star. However, if TTS SED is modified with a screen of foreground extinction, the near-infrared SED for CB54YC1-I can be reproduced with a class II pre-main sequence model. In Figure 4, as was done for CB54YC1-II, the median TTS SED (D'Alessio et al. 1999) has been scaled and convolved with an extinction model and fitted to the JHK data for CB54YC1-I. For a best-fit extinction of $A_V = 15 - 17$ mag, the TTS SED can reproduce the near-infrared data. However, the model predicts mid-infrared densities ($F_\nu \sim 20-40$ mJy at 11.7 μm and $F_\nu \sim 50-70$ mJy at 18.3 μm). The predicted mid-infrared emission for the TTS SED is $\sim 7\sigma$ above the detection limits.

It is possible that CB54YC-I is a more evolved star embedded in the globule or simply a star background to the globule. To explore these possibilities, we have fitted the JHK photometry with a blackbody function modified by a line-of-sight extinction curve: $S_\nu = \Omega B_\nu(T) \exp\left(-\mathrm{A}_\nu/1.086\right)$, where $B_\nu(T)$ is the Planck function, A_ν is the frequency-dependent extinction, and Ω is the solid angle. At each extinction value in the range from $A_V = 0 - 30$ mag ($\Delta A_V = 0.1$ mag), a range of temperatures ($T = 500 - 50000$ K in steps of 100 K) were tested.

For a given extinction value, there is a unique blackbody temperature for which the chi-square is a minimum, but there is no global minimum representing a best fit the JHK data. The average temperature uncertainty for a given extinction value is ~ 500 K. In Figure 5, the resulting reduced chi-squares and temperatures for each of the trial extinctions are plotted. The fitting uncertainty in the temperature for a given extinction value is approximately 10%. The reduced chi-square curve is relatively flat between $0 \leq A_V \leq 26$ mag. Beyond $A_V = 26$ mag, the reduced chi-square climbs above $\chi^2_\nu \approx 1$ and begins to diverge rapidly. The best fit temperature at this boundary is $T \approx 30000$ K. Because of the rapid change in the chi-square beyond this point, we regard this as the upper bound for the extinction and source temperature of CB54YC1-I.

The lower bound to the extinction and temperature is constrained only by the detection limits of the mid-infrared observations. The combination of temperature and extinction must be such that CB54YC1-I is not detected in all three mid-infrared filters (N, Si-11.7, & Qa-

18.3). For example, at zero extinction ($A_V = 0$ mag), the best fit temperature is $T \approx 1100$ K and the reduced chi-square is $\chi^2_\nu < 1$, but the predicted mid-infrared flux densities violate the non-detections at both N and 11.7 μm (see Figure 4).

The blackbody plus extinction models only predict mid-infrared flux densities below the detection limits in all three mid-infrared filters if $A_V \gtrsim 23$ mag. As an example, the predicted N-band flux densities (the most sensitive of the three observations) are plotted as a function of visual extinction in Figure 5 (*bottom*), showing that the predicted flux density drops below the detection limit at $A_V \gtrsim 23$ mag. We, therefore, regard $A_V \approx 23$ mag and the corresponding temperature ($T \approx 6000$ K) as the lower bound for CB54YC1-I. The lower ($A_V = 23$ mag, $T = 6000$ K) and upper ($A_V = 26$ mag, $T = 30000$ K) bounds for the blackbody model fits to CB54YC1-I are shown in Figures 4.

If the extinction is $A_V = 23$ mag, the temperature ($T \approx 6000$ K) suggests that the CB54YC1-I could be an early-G or late-F star. A main sequence dwarf of this spectral type has an absolute K magnitude of $M_K \approx 2.7$ mag. With a measured K magnitude of $K = 11.76$ (Yun 1996), the implied distance is only ~ 250 pc, much too close to be extinguished by CB54. If, however, CB54YC1-I is a G or F giant star, the star would be approximately 4.0 magnitudes brighter and located at a distance of ≈ 1500 pc, sufficiently distant to place CB54YC1-I behind the globule.

At the upper limit to the model fitting, ($A_V \approx 26$ mag, $T \approx 30000$ K), the temperature corresponds to a B0 star. With an estimated absolute magnitude of $M_K = -3$. CB54YC1-I would be at a distance of 2500 pc which is far enough to be behind the globule. The rarity and short lifespan (10 MYr) of B0 stars and the required chance alignment with the globule seem to make this a remote possibility.

If, instead, the extinction is near the middle of the extinction range ($A_V = 24 - 25$ mag), the best fit temperature ($T \approx 10000 - 15000$ K) implies that CB54YC1-I may be a young A or B star. With an absolute K magnitude of $M_K \approx -1.5 - 0$, this yields a distance of only $1200 - 1500$ pc placing CB54YC1-I at a distance consistent with being an embedded young star.

An alternative explanation for CB54YC1-I is that the source is an embedded protostar viewed at an extremely high inclination angle, and the near-infrared detections are not of the central protostar, but of light scattered by the accretion disk into our line of sight. Unfortunately, near-infrared photometry alone can not distinguish these models.

3.3. Mid-Infrared Sources

Three new sources have been detected by our mid-infrared observations. These sources have no near-infrared counterparts. The mid-infrared sources lie just beyond the edge of the shocked H_2 emission and do not correspond to any of the knots or condensations visible in the near-infrared diffuse emission (see Figure 1 and Yun 1996; Khanzadyan 2003). The mid-infrared sources, however, are located within the boundaries of the dense core in CB54 and clustered near the position of the IRAS point source (see Figure 1). The two brightest sources (MIR-a, MIR-b) were detected in all three filters, but MIR-c was detected only at 18.3 μm. A summary of the photometry is given in Table 2, and the SEDs for these sources are presented in Figure 6.

To characterize and understand the relative temperatures of the mid-infrared sources, a single temperature blackbody was fit to both MIR-a and MIR-b. The blackbody fits did not include the broad-band N (10.3 μm) flux density which are potentially contaminated with an unknown amount of amorphous silicate, and were fit to the narrow-band 11.7 μm and 18.3 μm flux densities. The best-fit blackbody (Figure 6) temperatures for the two sources are quite similar ($T_A = 110 \pm 10$ K and $T_B = 100 \pm 10$ K) and are near what is expected for the bolometric temperatures of class 0 protostars (André, Ward-Thompson, & Barsony 2000). If the N-band photoometry is included in the fits, the resulting temperatures increase by $10 - 20$ K.

Blackbody fits to the sub-mm and mm emission from the dense core yields a much colder envelope temperature of 25 K (Launhardt, Ward-Thompson, & Henning 1997). The summed flux densities predicted by the mid-infrared blackbody fits is not sufficient to explain the 100 μm flux density for IRAS PSC 07020-1618 ($F_\nu \approx 100$ Jy), indicating that these class 0 protostars are harbored within the cold, dense envelope.

If we assume that the mid-infrared emission is optically thin and little emission is contributed from the cold envelope, we can estimate the protostellar core mass associated with mid-infrared emission via

$$M_d = \frac{(16/3)\pi a \rho D^2}{Q_\nu B_\nu(T_d)} F_\nu \tag{1}$$

where F_ν is the observed flux density at frequency ν, Q_ν is the grain emissivity at frequency ν, a is the grain radius, ρ is the grain mass density, D is the distance to CB54, and B_ν is the Planck function at dust temperature T_d. Assuming $a = 0.5$ μm, $\rho = 1$ g cm^{-3}, $Q_\nu = 0.1(\lambda/\mu\mathrm{m})^{-\alpha}$, and $\alpha = 0.45$ (e.g., Muthumariappan, Kwok, & Volk 2006), we estimate dust masses for MIR-a and MIR-b of $M_a \approx 0.014$ $M_\odot$ and $M_b \approx 0.043$ $M_\odot$, respectively. For an average gas-to-dust mass ratio of 100, the central mid-infrared cores have masses of $M_a \approx 1.4$ $M_\odot$ and $M_b \approx 4.3$ $M_\odot$.

MIR-c was detected only at 18.3 μm, but if use the 11.7μm uppper limit to restrict the blackbody fitting, we find an upper limit to the temperature of 120 K. (see Figure 6). Coupled with the 18.3 μm flux density, we estimate a limit to the total mass (gas+dust) of $M_c \gtrsim 0.2\ M_\odot$.

4. Conclusions

We have obtained high angular resolution $10 - 18\ \mu$m imaging of CB54, a ~ 100 M$_\odot$ Bok globule known to harbor a dense core and two near-infrared sources previously classified as class I young stellar objects. We have detected only one (CB54YC1-II) of the two near-infrared sources, confirming its protostellar evolutionary status. Based upon the mid-infrared luminosity, we estimate that the central protostellar mass for CB54YC1-II is $M_* = 0.08 - 0.8\ M_\odot$, depending on the mass transfer rate. The SED is also consistent with a more evolved T Tauri star behind a screen of extinction. Without a more complete SED, it is not possible to distinguish between these models.

The other near-infrared source (CB54YC1-I) should have been detected if it were a class I protostar similar to that CB54YC1-II. We find that the near-infrared SED is consistent with the SED for a more evolved star extinguished by the globule itself. CB54YC1-I may be a background F- or G-giant or may be an embedded young A- or B-star. An alternative explanation for CB54YC1-I is that the source is an embedded protostar viewed at an extremely high inclination angle, and the near-infrared detections are not of the central protostar, but of light scattered by the accretion disk into our line of sight. High spatial resolution near-infrared polarimetry and/or mid-infrared spectroscopy could be used to ascertain the status CB54YC1-I. If CB54YC1-I is an embedded, young A or B star, its mass may be on the order of $\sim 2 - 5\ M_\odot$.

Additionally, we have discovered three new mid-infrared sources (MIR-a, MIR-b, and MIR-c) which are spatially coincident with both the position of the associated IRAS point source and the center of the dense core in CB54. These sources are characterized with a 100 K blackbody, consistent the expected bolometric temperature of a class 0 protostar. Based upon the mid-infrared emission, we have estimated the masses for these sources to be $\sim 4\ M_\odot$, $\sim 1.5\ M_\odot$, and $\sim 0.2\ M_\odot$.

If CB54YC1-I is indeed an embedded A or B star, it is interesting to speculate that CB54YC1-I may have formed first and induced star formation further in the cloud, through the interaction of its outflow/winds with remainder of the globule. The total mass estimated for the sources within CB54 is about $10 - 15$ M$_\odot$ or about $10 - 15\%$ of the total cloud mass.

Such a sequential process of star formation occurring in the Bok globule CB54 may be similar to what is observed in other globules (Huard, Weintraub, & Sandell 2000; Codella et al. 2006). Spectroscopy and a more complete SED in the mid-infrared and far-infrared is needed to disentangle the possible spectral types and evolutionary states for the sources in CB54.

These observations were carried out during payback time to C. Telesco for development of T-ReCS. The authors would like to thank Charlie Telesco, Chris Packham, and Margaret Moerchen for collecting these data. Portions of this work were supported by the California Institute of Technology under contract with the National Aeronautics and Space Administration. C. G. M. acknowledges support from a University of Florida Graduate Minority Fellowship, a SEAGEP Fellowship, and NSF grants AST97-3367 and AST 02-02976. C. G. M. would like to thank Eric McKenzie and Ana Matkovic for comments and suggestions. Based on observations obtained at the Gemini Observatory, which is operated by the Association of Universities for Research in Astronomy, Inc., under a cooperative agreement with the NSF on behalf of the Gemini partnership: the National Science Foundation (United States), the Particle Physics and Astronomy Research Council (United Kingdom), the National Research Council (Canada), CONICYT (Chile), the Australian Research Council (Australia), CNPq (Brazil) and CONICET (Argentina). This research has made use of the NASA/IPAC Infrared Science Archive, which is operated by the Jet Propulsion Laboratory, California Institute of Technology, under contract with the National Aeronautics and Space Administration.

REFERENCES

Afonso, J. M., Yun, J. L., & Clemens, D. P. 1998, AJ, 115, 1111

Alves, J. F. & Yun, J. L. 1995, ApJ, 438, L107

André, P. & Montmerle, Th. 1994, ApJ, 420, 837

André, P., Ward-Thompson, D., & Barsony, M. 1993, A&A, ApJ, 420, 837

Andre, P., Ward-Thompson, D., & Barsony, M. 2000, Protostars and Planets IV, 59

Bontemps, S., André, P., Terebey, S., & Cabrit, S. 1996, A&A, 311, 858

Bourke, T. L., Hyland, A. R., & Robinson, G. 1995, MNRAS, 276, 1052

Ciardi, D. R., Telesco, C. M., Williams, J. P., Fisher, R. S., Packham, C., Piña, R., & Radomski, J. 2003, ApJ, 585, 392

Ciardi, D. R., Telesco, C. M., Packham, C., Gómez Martin, C., Radomski, J. T., De Buizer, J. M., Phillips, C. J., & Harker, D. E. 2005, ApJ, 629, 897

Clemens, D. P. & Barvainis, R. 1988, ApJS, 68, 257

Clemens, D. P., Yun, J., & Heyer, M. 1991, ApJS, 75, 877

Codella, C., Brand, J., Massi, F., Wouterloot, J. G. A., & Davis, G. R. 2006, A&A, 457, 891

D'Alessio, P., Calvet, N., Hartmann, L., Lizano, S., & Cantó, J. 1999, ApJ, 527, 893

de Gregorio-Monsalvo, I., Gómez, J. F., Suárez, O., Kuiper, T. B. H., Anglada, G., Patel, N. A., & Torrelles, J. M. 2006, AJ, 132, 2584

Eisner, J. et al. 2006, ApJ635, 396

Furuya, R. S., Kitamura, Y., Wootten, H. A., Claussen, M. J., & Kawabe, R. 2001, ApJ, 559, L143

Gómez, J. F., de Gregorio-Monsalvo, I., Suárez, O., & Kuiper, T. B. H. 2006, AJ, 132, 1322

Haisch, K. E., Jr., Lada, E. A., & Lada, C. J. 2000, AJ, 120, 1396

Henning, Th., Wolf, S., Launhardt, R. & Waters, R. 2003, ApJ, 561, 871

Huard, T. L., Weintraub, D. A., & Sandell, G. 2000, A&A, 362, 635

Jayawardhana, R., Hartmann, L. & Calvet, N. 2001, ApJ, 548, 310

Kenyon, S. J., Calvet, N., & Hartmann, L. 1993, ApJ, 414, 676

Khanzadyan, T. 2003, Ph.D. Thesis

Launhardt, R. & Henning, Th. 1997, A&A, 326, 329

Launhardt, R., Ward-Thompson, D., & Henning, Th. 1997, MNRAS, 288, L45

Masunaga, H. & Inutsuka, S. 2000, ApJ, 531, 350

Mathis, J. S. 1990, ARA&A, 28, 37

Moreira, M. C. & Yun, J. L. 1995, ApJ, 454, 850

Moreira, M. C., Yun, J. L., Vázquez, R. & Torrelles, J. M. 1996, AJ, 113, 1371

Muthumariappan, C., Kwok, S., & Volk, K. 2006, ApJ, 640, 353

O'Linger, J. C., Cole, D. M., Ressler, M. E., & Wolf-Chase, G. 2006, AJ, 131, 2601

Rebull, L. et al. 2007 in press

Saraceno, P., André P., Ceccarelli, C., Griffin, M., & Molinari, S. 1996, A&A, 309, 827

Shu, F. H., Adams, F. C., & Lizano, S. 1987, ARA&A, 25, 23

Stahler, S., Shu, F. H., & Taam, R. E. 1980, ApJ, 242, 226

Telesco, C. M., Piña, R. K., Hanna, K. T., Julian, J. A., Hon, D. B., & Kisko, T. M. 1998, SPIE, 3354, 534

Wang, Y., Evans, N. J., II, Zhou, S., & Clemens, D. P. 1995, ApJ, 454, 217

Yun, J. L. 1996, AJ, 111, 930

Yun, J. L. & Clemens, D. P. 1990, ApJ, 365, L73

Yun, J. L. & Clemens, D. P. 1994a, AJ, 108, 612

Yun, J. L. & Clemens, D. P. 1994b, ApJS, 92, 145

Yun J. L., Moreira M. C., Torrelles J. M., Afonso J. M., & Santos N. C., 1996, AJ, 111, 841

Zhou, S., Evans, N. J. II, & Wang, Y. 1996, ApJ, 466, 296

This preprint was prepared with the AAS LaTeX macros v5.2.

Table 1. Summary of Observations

Filter	λ_c (μm)	$\Delta\lambda$ (μm)	Frame Time (ms)	On-Source (seconds)	Air Mass
N	10.36	5.27	25.8	304	1.11
Si-11.66	11.7	1.13	25.8	304	1.84
Qa-18.30	18.3	1.51	25.8	912	1.18-1.34

Table 2. Source Positions and Flux Densities

Source	$(\Delta\alpha,\ \Delta\delta)$[a]	J 1.22 μm (mJy)	H 1.65 μm (mJy)	K 2.18 μm (mJy)	MSX-A 8.28 μm (mJy)	N 10.36 μm (mJy)	Si-11.7 11.66 μm (mJy)	Qa-18.3 18.3 μm (mJy)	References
YCII	$(0.0, 0.0)$	0.71 ± 0.07	5.56 ± 0.56	37.3 ± 3.7	278 ± 19	302 ± 5	217 ± 6	431 ± 11	1,2
YCI	$(-10.0, +8.3)$	0.59 ± 0.06	4.63 ± 0.46	12.9 ± 1.3	···	< 4	< 6	< 10	1,2
MIR-a	$(-15.8, +1.7)$	···	···	···	···	16 ± 4	14 ± 6	219 ± 11	2
MIR-b	$(-13.6, -1.8)$	···	···	···	···	12 ± 4	14 ± 6	322 ± 11	2
MIR-c	$(-12.6, -3.8)$	···	···	···	···	< 4	< 6	70 ± 12	2

[a] Positional offsets in arcsec from the source CB54YC1-II ($\alpha = 07h04m21.7s,\ \delta = -16^\circ 23' 19''$ (J2000)).

References. — 1. Yun (1996); 2. This Work

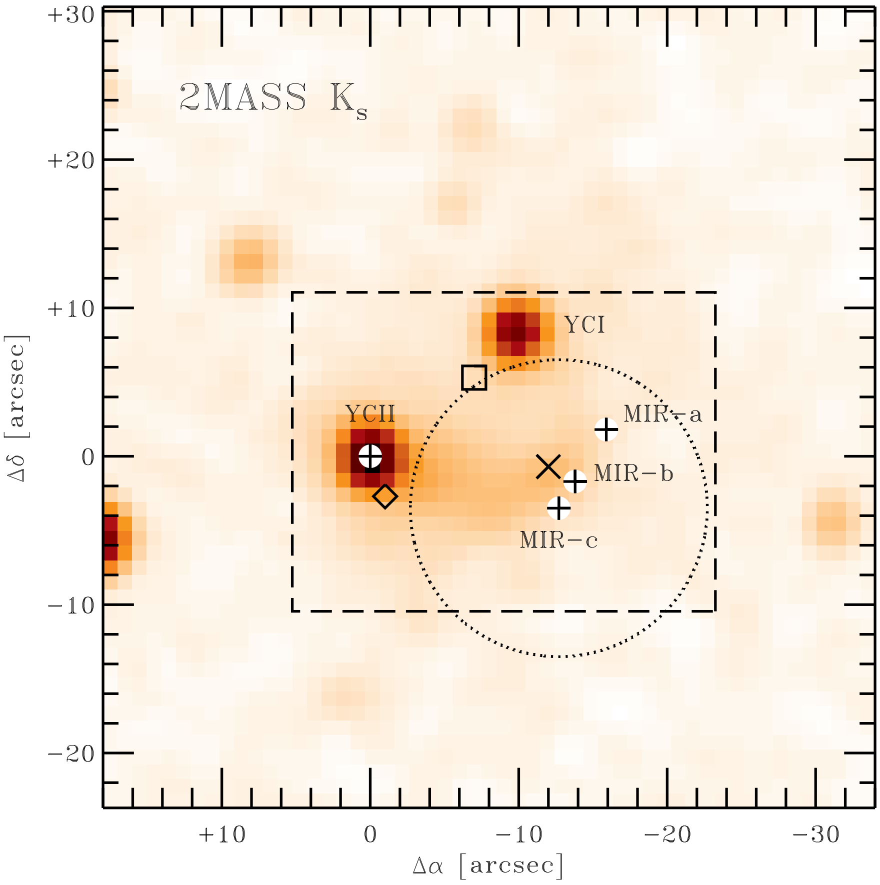

Fig. 1.— 2MASS K_S image of CB 54. The dashed line delineates the area imaged with T-ReCS. The near-infrared sources CB54YC1-I and CB54YC1-II are annotated, and the positions of the detected mid-infrared sources are marked with the filled white circles (see Figure 2). The image (0,0) position is centered on CB54YC1-II. The circle (dotted line) is centered on the peak of 850 μm core; the size of the circle represents the approximate size of the 850 μm core (Henning et al. 2001). The cross marks the position of the IRAS source PSC 07020-1618. The open diamond marks the position of the 8 μm MSX source G228.9946-04.6200, and the open square marks the position for the cm source discovered with the VLA (Yun et al. 1996). The image pixel scale is $1''$ pix^{-1}.

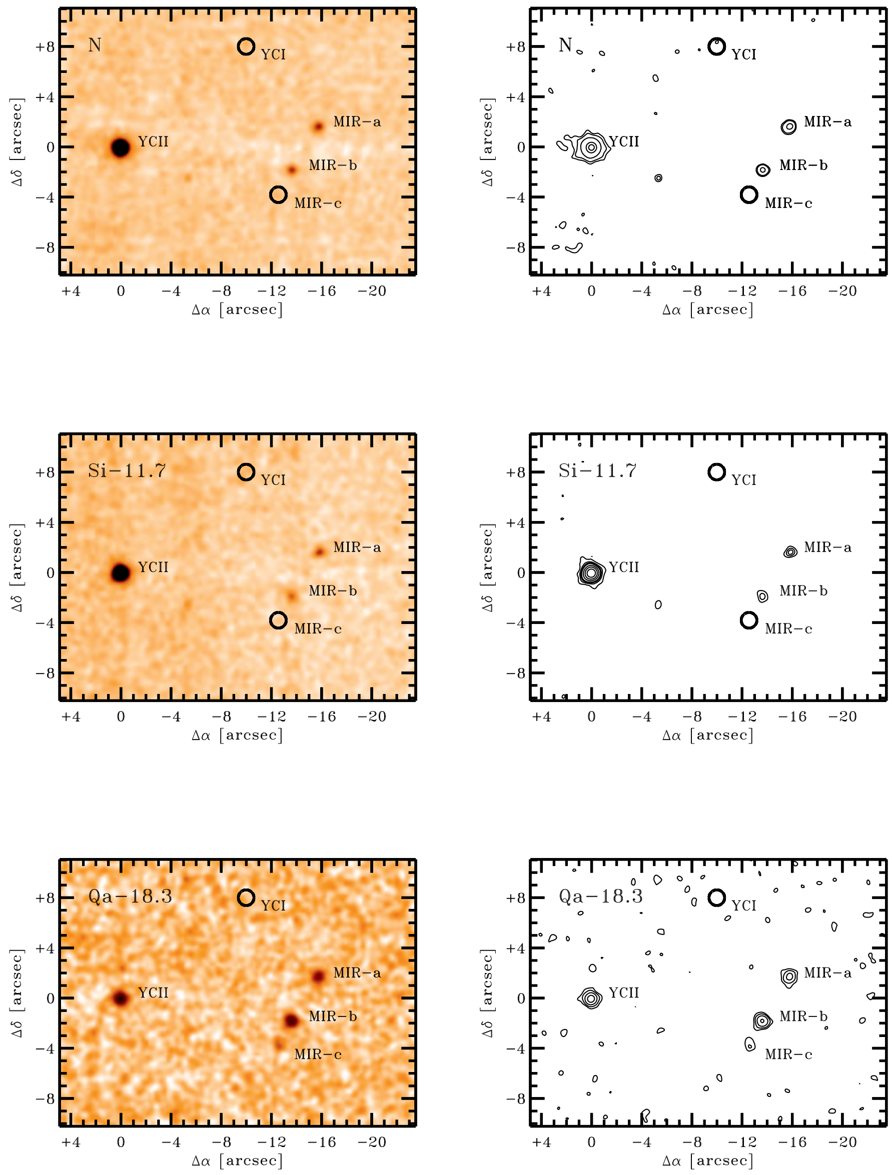

Fig. 2.— T-ReCS N-band, 11.7μm and 18.3μm images and contour plots of CB54. The (0,0) point of each image is centered on CB54YC1-II. The images have been stretched by an inverse hyperbolic sine to enhance the contrast. The detected mid-infrared sources are annotated. The position of CB54YC1-I (not detected by the mid-infrared observations) is marked in each image, and the position of MIR-c (detected only at 18.3μm) is marked in the N-band and 11.7μm images. The N-band contour levels are $[0.03, 0.05, 0.15, 1.5, 3.5]$ mJy pix^{-1}; the 11.7 μm contour levels are $[0.05, 0.10, 0.15, 0.2, 0.4, 0.8, 1.6]$ mJy pix^{-1}; the 18.3 μm contour levels are $[0.4, 0.8, 1.6, 3.2]$ mJy pix^{-1}. The pixel scale for each image is $0\farcs089$ pixel^{-1}.

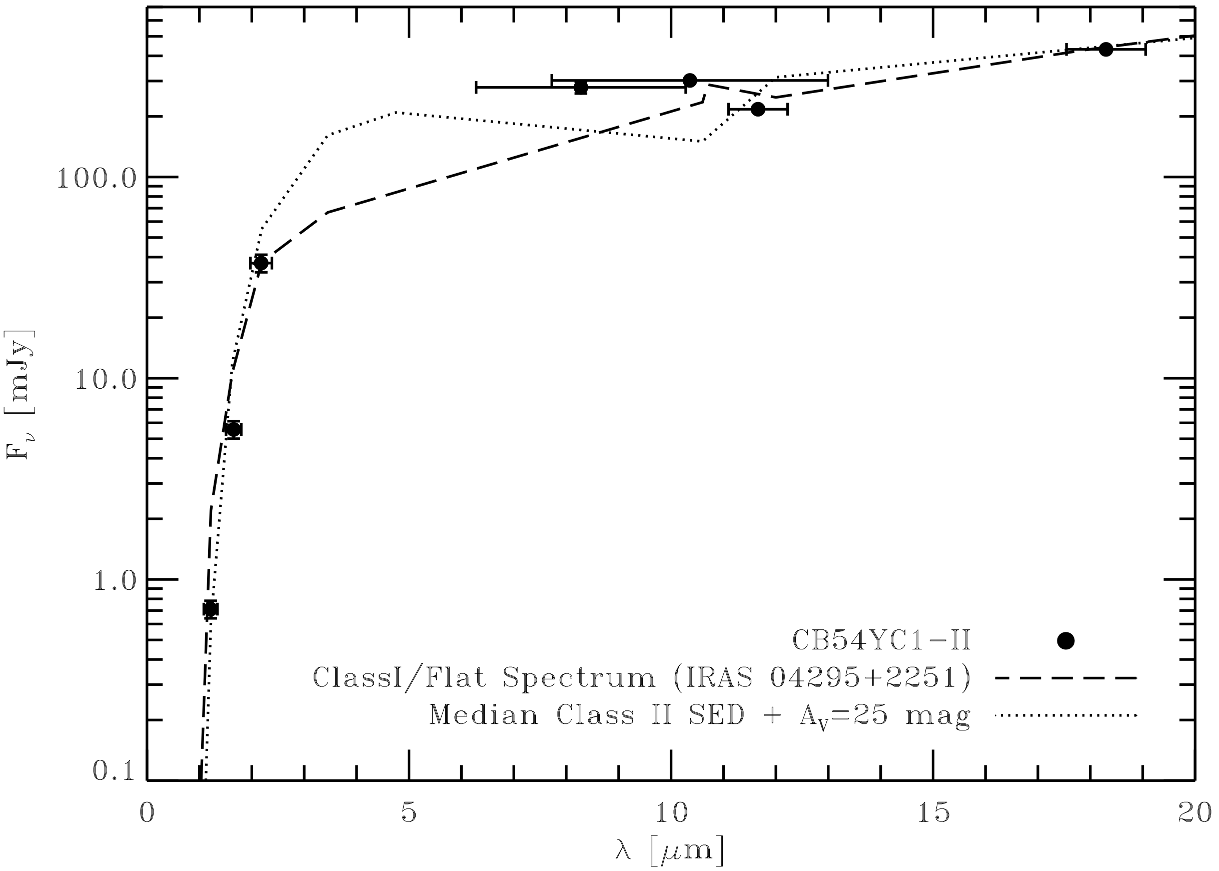

Fig. 3.— The SED of CB54YC1-II (solid points). The horizontal error bars represent the bandwidth of the filters. The dashed line represents the SED for the class I protostar IRAS 04295+2251. The dotted line represents a median TTS SED convolved with $A_V = 25$ magnitudes of extinction.

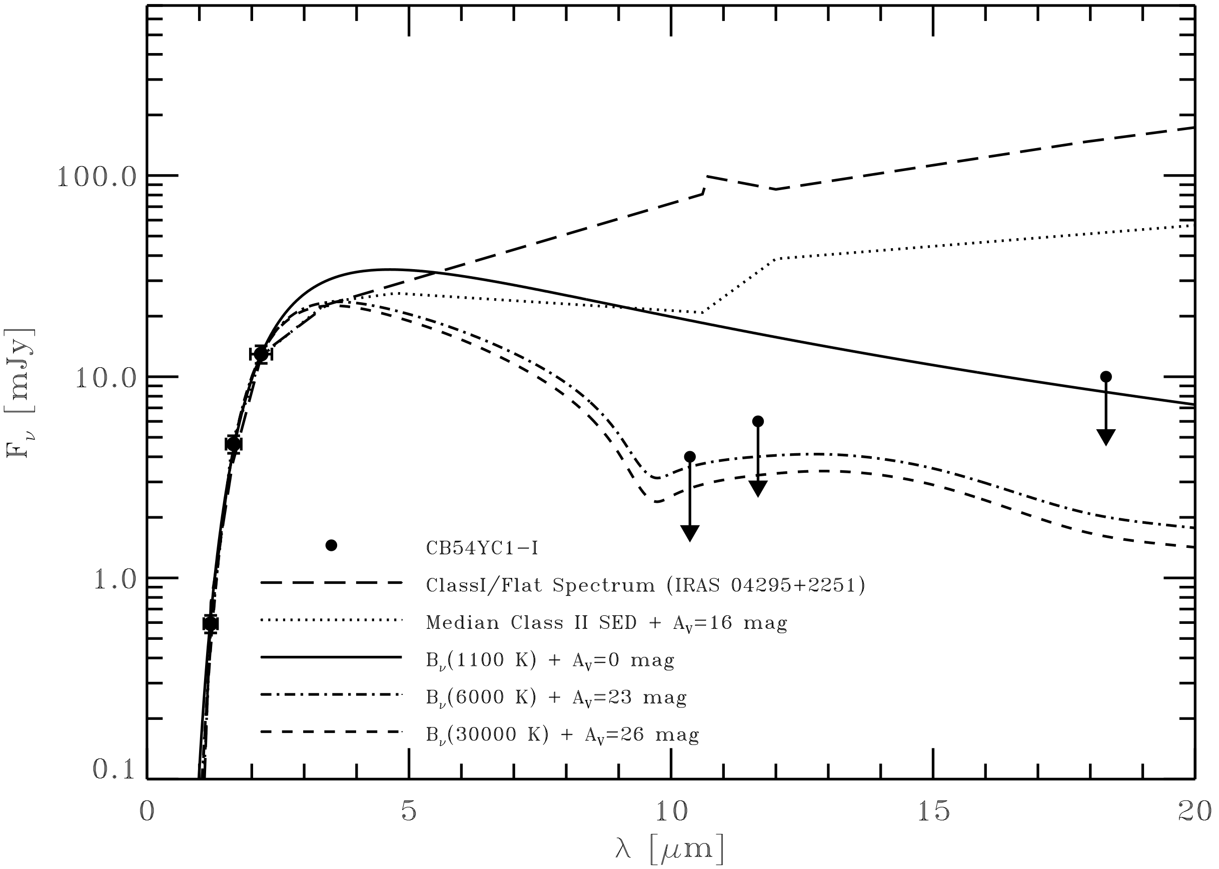

Fig. 4.— The SED of CB54YC1-I (solid points). Upper limits for the mid-infrared observations are represented by the downarrows. The long-dashed line represents the SED for the class I protostar IRAS 04295+2251. The dotted line represents a median TTS SED convolved with $A_V = 16$ magnitudes of extinction. The solid line is a 1100 K blackbody; the dash-dot line is a 6000 K blackbody convolved with $A_V = 23$ magnitudes of extinction, and the short-dashed line is a 30000 K blackbody convolved with $A_V = 26$ magnitudes of extinction.

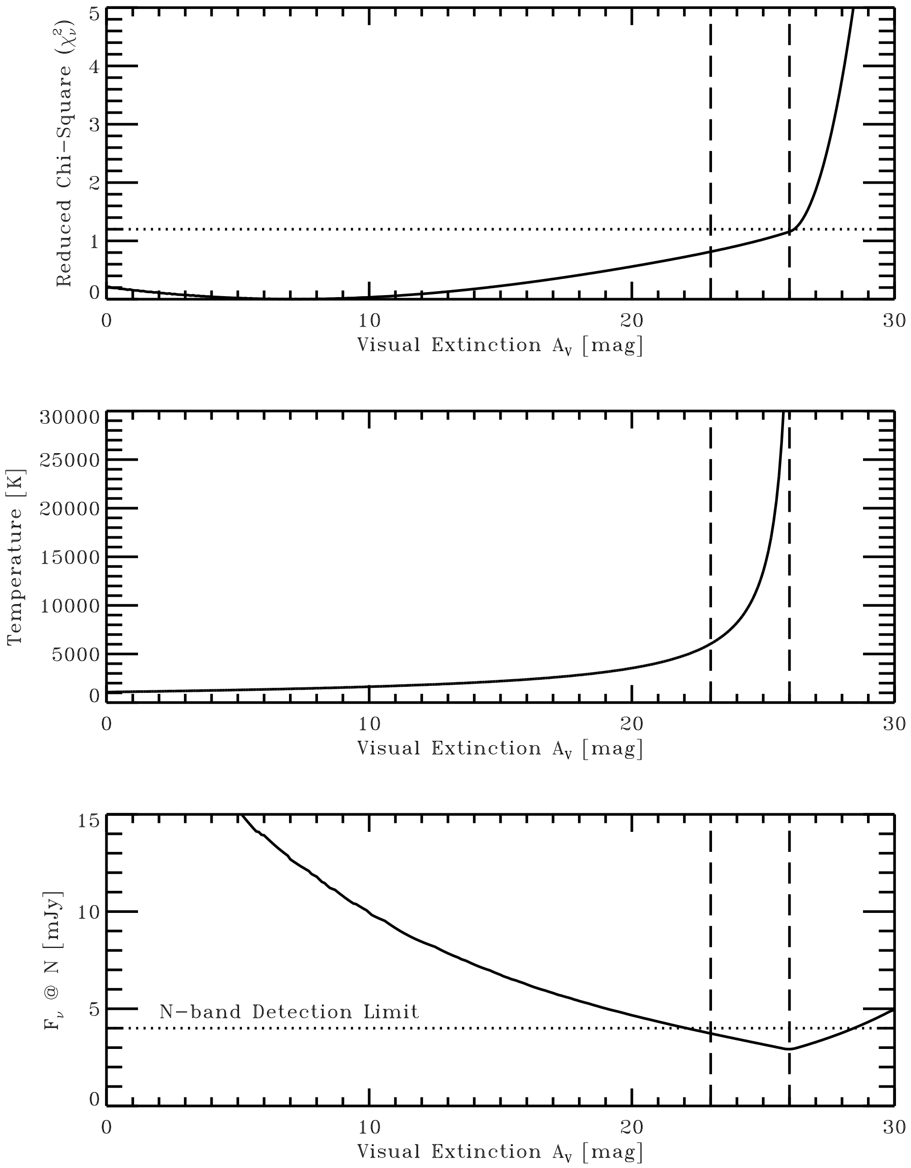

Fig. 5.— Reduced chi-squares (*top*), best-fit temperatures (*middle*), and predicted N-band flux densities (*bottom*), are plotted as a function of visual extinction for the black-body+extinction models fitted to the JHK flux densities of CB54YC1-I. The horizontal dashed line in the chi-square plot marks the sharp knee in the chi-square curve at $A_V = 26$ mag ($\chi^2_\nu = 1.2$). The horizontal dashed line in the flux density plot marks the 1σ detection limit (4 mJy) of the N-band observations. The vertical dashed lines delineate the extinction range of $23 \leq A_V \leq 26$ mag (see text for details).

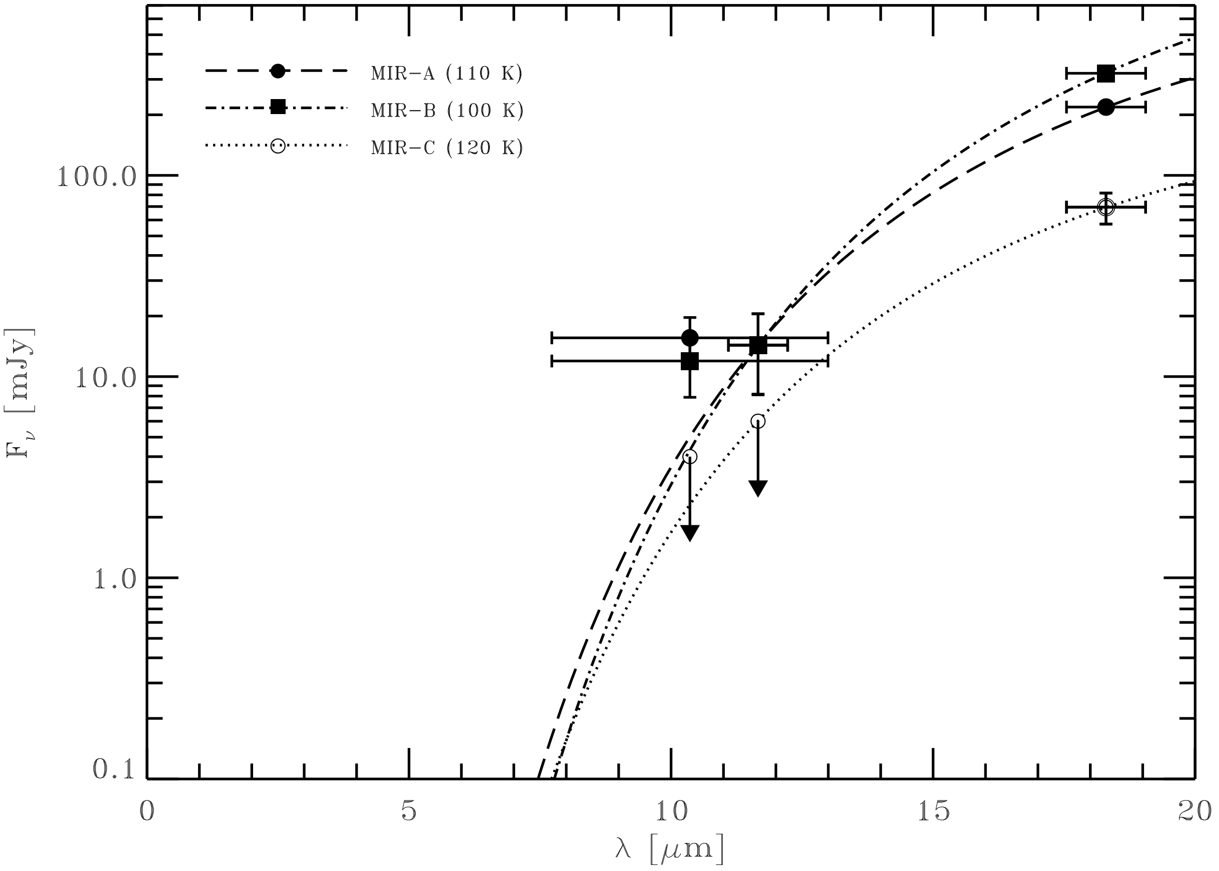

Fig. 6.— The SEDs of the mid-infrared sources MIR-a (solid squares), MIR-b (solid circles), and MIR-c (open circles). The 110 K and 100 K best-fit blackbody curves are shown for MIR-a (dashed) and MIR-b (dot-dash). For MIR-c, the dotted line represents a 120 K blackbody which is fit to the 18.3μm flux density and the 11.7μm upper limit. The horizontal error bars represent the bandwidth of the filters.